Robotica (2005) volume 23, pp. 419–434. © 2005 Cambridge University Press
doi:10.1017/S0263574704000852 Printed in the United Kingdom

Development of mobile versatile nanohandling microrobots: design, driving principles, haptic control

A. Kortschack*, A. Shirinov, T. Trüper and S. Fatikow

University of Oldenburg, Division Microrobotics and Control Engineering, Oldenburg (Germany)

SUMMARY

Special micromanipulators are needed to manipulate very small objects. Most micromanipulators are specialized to perform a task they are designed for, but are too inflexible to adapt to other problems. Therefore, flexible newly developed mobile microrobots are presented with precision in the sub-micrometer range while offering a macroscopic workspace. The main parts of each mobile microrobot, the mobile platform, the manipulator and end effectors, are explained in detail, with some experimental data given.

The new driving principle of the mobile platform allows high resolution, low energy consumption, which makes an on-board power supply feasible and a maximum velocity of several mm/s.

Useful human interfaces are needed for a successful teleoperation. The most important interface next to the vision feedback is a haptic interface. The paper presents a newly developed haptic interface for a micromanipulation station. The mechanical design and the design of the control system of the haptic interface are discussed in details. The control architecture of the micromanipulation station and the integration of the haptic device into the micromanipulation station are presented.

KEYWORDS: Haptic control; Microrobots; Nanohandling; Microassembly.

1. INTRODUCTION

The development of microrobots for the manipulation of objects on the micrometer scale is not easy. The robotic research community has been doing research on that field for many years now.[1–6] There is still a lack of flexible, easy to use micromanipulators. The main focus of development is to create micromanipulators capable of suitable, flexible, highly precise and fast operation.

The authors' contribution to that field is the development of mobile microrobots using new, smart and highly precise direct drives. These mobile robots perform manipulation tasks with a nanometer range precision and transport objects at speeds of up to several mm/s over distances of a few hundred millimetres. Because of the mobility, which guarantees modularity and flexibility, the microrobots can be used for diverse applications. The intention while developing a nanohandling robot cell (figure 1) is to enable an operator to perform even difficult manipulation tasks with several specialized mobile microrobots which can work together. Each of the mobile microrobots can easily be teleoperated by use of visual feedback in combination with an haptic interface.

By using an optical microscope, manipulation processes with micrometer precision can be carried out. To realize manipulation tasks in the nanometer range the mobile microrobots will have to work in the vacuum chamber of a scanning electron microscope (SEM).

Not every type of actuator is suitable to drive the microrobot's components. First of all, the actuators have to guarantee highest and controllable accuracy to enable the microrobot to perform precise manipulation tasks in the nm-rage. The actuator material should allow a simple mechanical structure, like direct force- and torque-transmission, to reduce disturbing influences like friction or slackness. A predictable behaviour is essential for a reasonable integration in a control system. The whole microrobot's size should not exceed a few cm^3. Therefore the dimensions of the actuator have to be small, thus requiring a high work density. A fast response of the actuator is needed, not only for quick motion, but also for a rapid compensation of disturbing influences.

Because the degree of miniaturization is increasing rapidly, microassembly is an important application. Hybrid microsystems for example are extremely difficult to assemble in comparison to monolithic microsystems. These hybrid microsystems need advanced microassembly techniques.

In nanotechnology research often complex manipulation tasks have to be performed. Therefore a flexible manipulation system is needed, which is able to perform a variety of nanomanipulation tasks with an adequate precision to realize advanced experiments.[7–9]

Advanced micromanipulation tasks are required for quality control in the semiconductor industry. In the field of material research advanced micromanipulators are needed to realize tests like nanoindentation and nanoscratching, essential to evaluate thin films. Micromanipulators are also needed in the fields of biological and medical research. Typical applications are in vitro fertilisation, the development of pharmaceutics and genetic research. The first applications of the microrobots are simple manipulation tasks with cell-like objects. Those experiments are described in section 3.

Until now the microrobots are teleoperated. One of the most important user interfaces is the haptic interface. Therefore a haptic interface with force feedback in several

* Corresponding editor: E-mail: kortschack@informatik.uni-oldenburg.de

https://doi.org/10.1017/S0263574704000852 Published online by Cambridge University Press

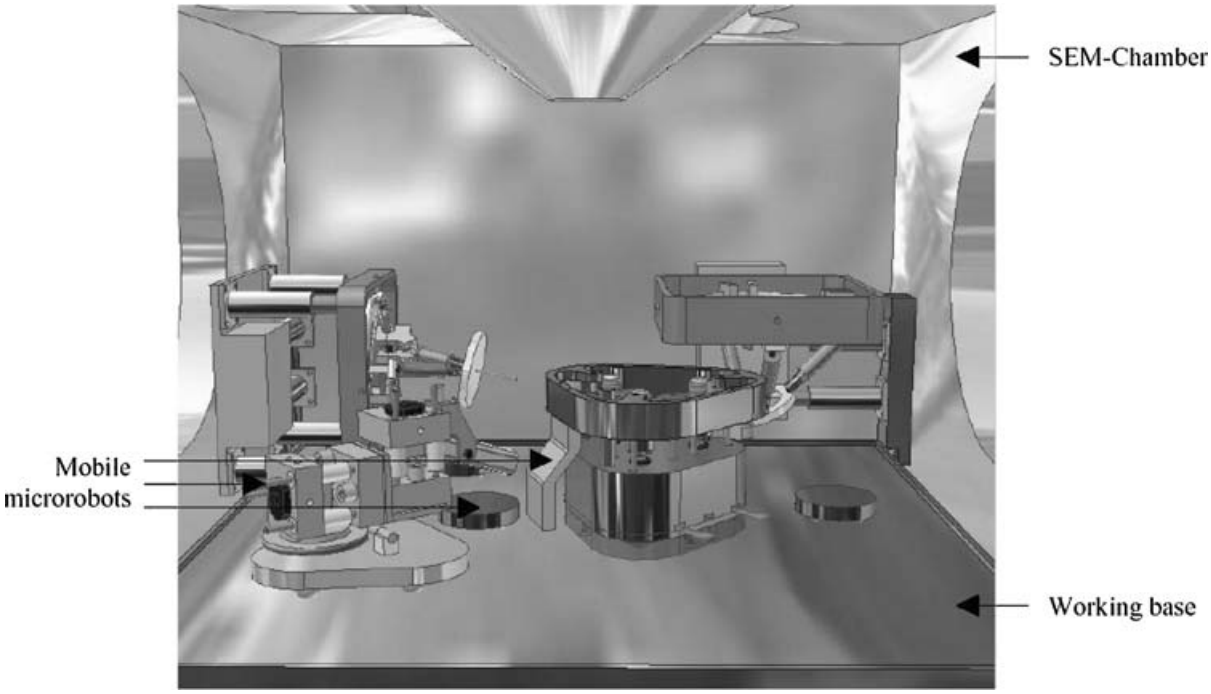


Fig. 1. Concept of a nanohandling robot cell inside a scanning electron microscope.

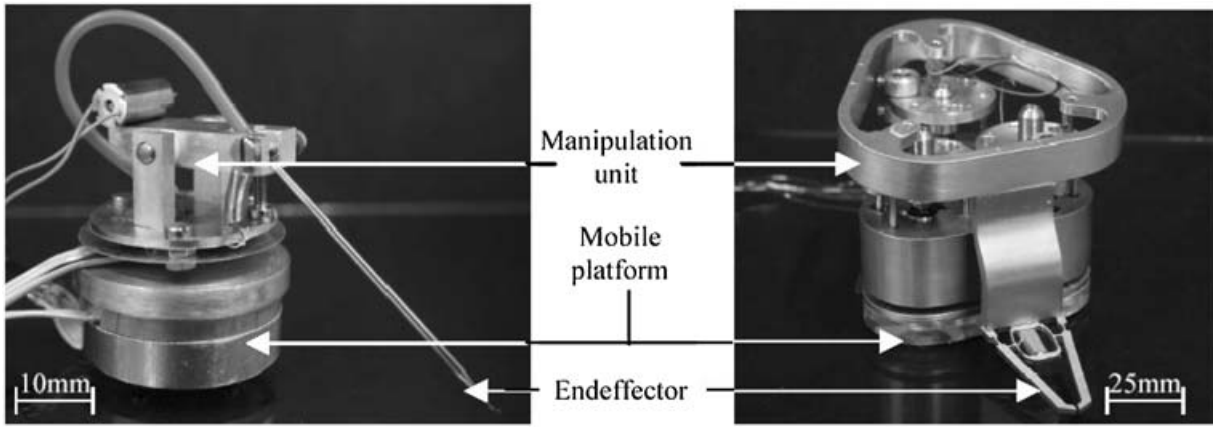


Fig. 2. Mobile microrobots (RollBot III and RollBot IV).

DOF has been developed, especially designed for micromanipulation with mobile microrobots.

The developed haptic interface introduces a unique design for the comfortable teleoperation of microrobots and a nanohandling station. This paper presents the mechanical design of the developed haptic interface, the design of its control system, and describes the integration of this haptic interface into the nanohandling station.

2. MOBILE MICROROBOTS

Mobile microrobots are able to move with 3-DOF on a working plane. The area of work is only restricted by the dimension of that plane and by the length of the wires connected to the microrobots. Because of that flexibility the robots are able to reach a manipulation assembly site from all required sides by moving around the setup. Only the currently required mobile microrobots are working at the manipulation site. All other mobile microrobots can be steered out of the way, so that there is enough working space for those microrobots involved in the manipulation. The mobility of the microrobots allows the change of tools at a remote place and the transportation of material to be manipulated.

The mobile microrobot consists of three main parts, a mobile platform, a manipulation unit and special end-effectors (figure 2).The modular concept of the microrobots allows the exchange of mobile platforms, manipulators and end-effectors, depending on the tasks the microrobots have to perform. In general, the component can be exchanged without additional tools. The microrobots are robust enough for manual handling.

2.1. Mobile platform

The task of the mobile platforms is to transport the manipulation unit and the end effectors to the site of the manipulation. Therefore the platform must have the three DOF to move freely on the working base. The mobile platforms have to achieve a precision in the high nanometer range. To reduce

https://doi.org/10.1017/S0263574704000852 Published online by Cambridge University Press

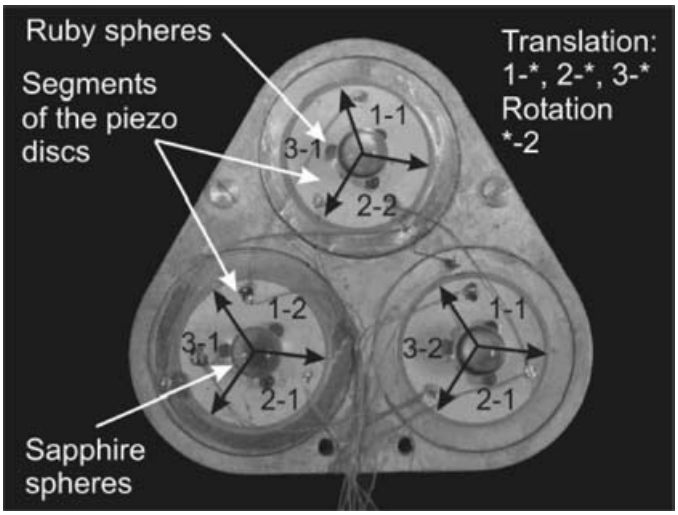


Fig. 3. Segmented piezo discs.

auxiliary process time, the platform has the ability to move with a velocity of several mm/s. The mobile platform has to carry the manipulation unit and end effectors, with a combined mass from 15 g to more than 500 g, depending on the task and the type of the mobile robot.

The mobile platforms are driven by the slip-stick principle.[10–12] The functional material for the actuators is piezoelectric ceramic in form of piezo discs, commonly used in piezo buzzers. The discs are segmented to create several electrodes per disc. (figure 3).

The segments of the discs are created by mechanical scratching, or alternatively by etching the upper electrode with nitric acid. One ruby ball is glued onto each segment. In the centre of the triangle formed by the ruby balls a steel or sapphire sphere is placed. The segments of each piezo disc can be bent by a voltage. In figure 4, a sequence of a clockwise rotation of a sphere is shown.

The segments can be bent by supplying a voltage. By a slow bending of a piezo disc segment the sphere can be rotated in the desired direction. When the voltage signal changes fast, the piezo segment is bent fast as well. During that fast movement, the ruby ball slips over the surface of the sphere. The sphere cannot follow that movement, because of its inertia. After that the segment is bent slowly back in its original position. During this slow movement the sphere performs a small rotation again. By repeating this sequence with a high frequency the spheres can be rotated with several revolutions per second. To drive this kind of actuator, a sawtooth voltage signal is required. This mode of movement can be used for coarse positioning.

Not investigated yet, but promising for the realization of fine positioning is the slow bending of the segments. It is assumed, that during the fine positioning in the horizontal plane, the platform is drifting in the vertical direction as well, which would be problematic.

In the following two slightly different mobile platforms are explained. The first mobile platform has three segmented piezo discs integrated in its underside, which allow a translation and rotation of the mobile platform. This platform has some advantages compared to other known mobile platforms driven by the slip-stick-principle.[11–16] All these platforms require wear-resistant surfaces to prevent damage of the working base. The new described platforms are less damaging to the surface, because the rapidly moving ruby balls have no direct contact with the surface anymore, but only with the spheres which are rolling over the surface. The spheres have to be made of hard materials, like steel, ceramics or sapphire because of the high frequency movements of the ruby balls on their surfaces. But there is no need of especially robust materials for the working surface: because the spheres are rolling over the surface, the smoothness of the working base it not that important any more, whereas usually the slip-stick-drive requires very smooth surfaces.[17] This enables the robot to drive on a variety of surfaces like steel, glass, plastic and even on paper.

Most slip-stick-driven platforms require high driving voltages in the range of 100 V or more to achieve reasonable movements. The new platform is driven by a voltage between 5–60 V, depending on the thickness of the piezo disc. Therefore, it is possible to use less expensive amplifiers. The circular blank of the thicker disc has gauge of 0.4 mm. Its piezo layer has a thickness of 0.2 mm. For this kind of piezo 30 V or more should be used to drive the mobile platform. The circular blank of the thinner disc has 0.2 mm and the piezo layer 0.1 mm.

The forces, needed for the micromanipulation, vary from several μN up to a few hundred mN. The mobile platform is able to pull and push objects with a force up to 0.3 N, depending on the weight placed on the platform (figure 5), which is strong enough for many micromanipulation tasks.

The working space under a light microscope or inside the vacuum chamber of an SEM is restricted (figure 1). The aim is to enable the cooperation of several mobile robots in such a confined working space. Therefore the robots have to be as small as possible. To realize further miniaturization, the components of the mobile platform need a different

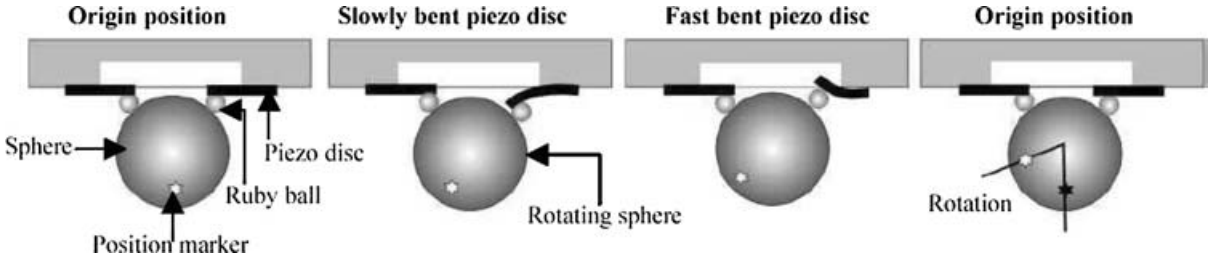


Fig. 4. Slip-stick-drive for the spheres.

https://doi.org/10.1017/S0263574704000852 Published online by Cambridge University Press

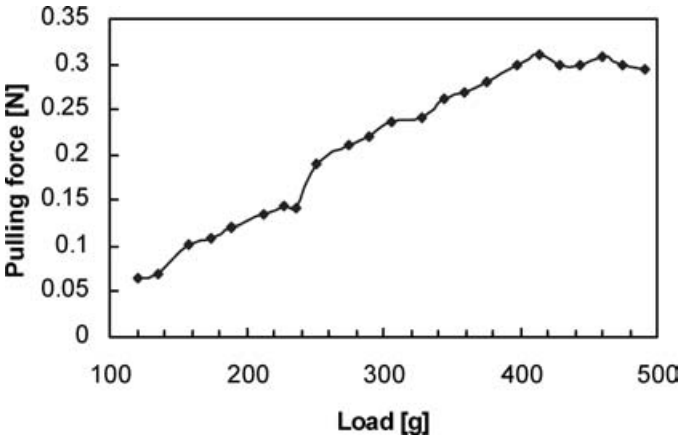


Fig. 5. Ability of the platform to pull and push objects depending on its weight.

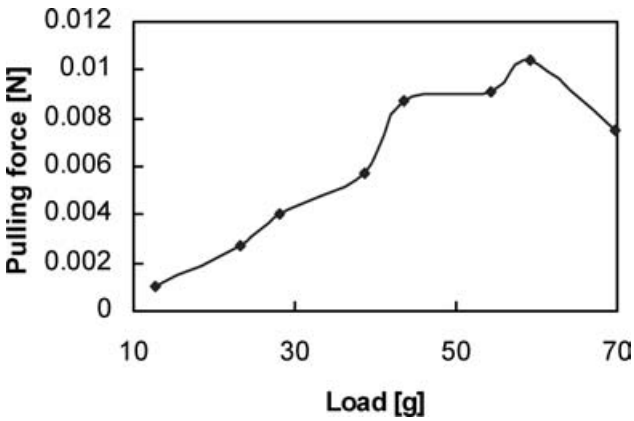


Fig. 7. Ability of the smaller platform to pull and push objects depending on it's weight.

configuration. Instead of using three piezo discs, one disc has been segmented as shown in figure 6 with one possible arrangement of the channels shown as well. This platform can be driven by low voltages in the range of 20–40 V.

The forces the smaller platform can exert are not nearly as high as the forces of the bigger one, as shown in figure 7. The maximal velocities, which differ as well, are shown in figure 8.

The high precision is the platform's most important feature. As already mentioned, two different operating states, the coarse and fine positioning mode, have to be well-defined. The precision of the coarse positioning mode equals the minimal rotation of the spheres during one period of the sawtooth driving signal. The fine positioning can be achieved by slowly bending the different piezo segments by a quasi-static voltage.

As shown in figure 9, the minimum step width for the smaller platform in the coarse positioning mode is approximately 110 nm.

For this experiment, an SEM test sample (CHESSY – Plano W. Plannet GmbH) was placed on top of the mobile platform. One SEM picture was taken before a single step. Then a single step was performed by supplying one period of a sawtooth signal of an amplitude of 5 V. After that step the second SEM picture was taken. The structure of the SEM test sample was used to measure the performed step length.

By supplying a quasi static voltage to the piezo segments, the test object can be shifted within the limits of the SEM's resolution. But the use of this kind of fine positioning mode has to be questioned. It is uncertain if this way of fine positioning is working acceptably, because the bending of the segments will not only cause a horizontal movement, but a vertical movement as well. This assumed drawback must be investigated further. Therefore, the mobile platform should only be used for coarse positioning in the range of a few hundred nanometers, if a manipulation unit is mounted on top.

The smaller mobile platform has a weight of only 12 g. As shown in figure 8, the pulling force of the platform is quite low as well. Unfortunately, seven electrical wires are necessary to drive this platform. These wires have a strong influence on the platform's motion as long as no extra weight is put on the platform. Therefore some efforts have to be made to reduce the number of wires. A first step is the integration of an on-board power supply. The energy consumption of both platforms is quite low: approximately 0.8 W. The power consumption has been measured at full load, which means

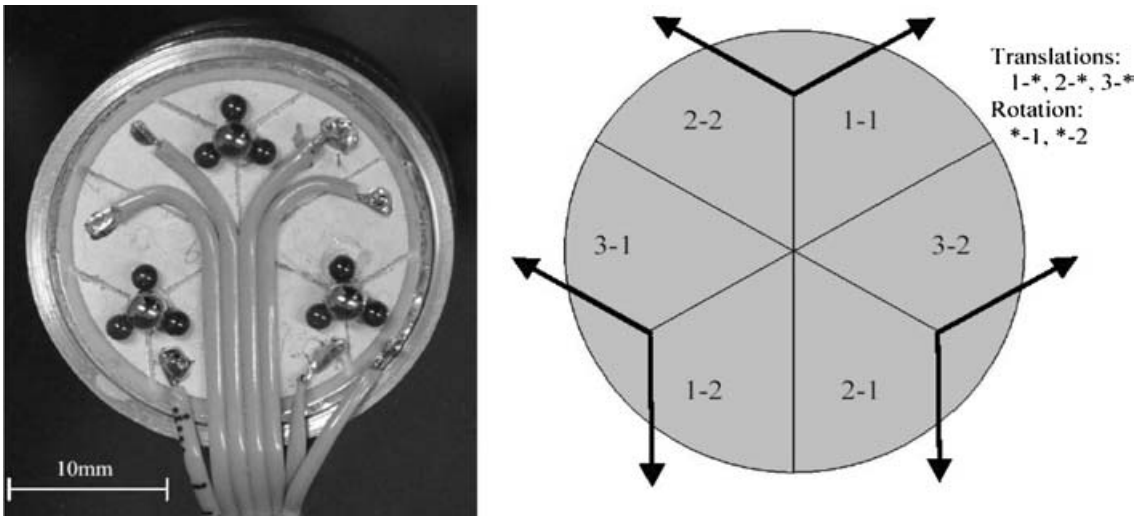


Fig. 6. Small mobile platform and its segmentation.

https://doi.org/10.1017/S0263574704000852 Published online by Cambridge University Press

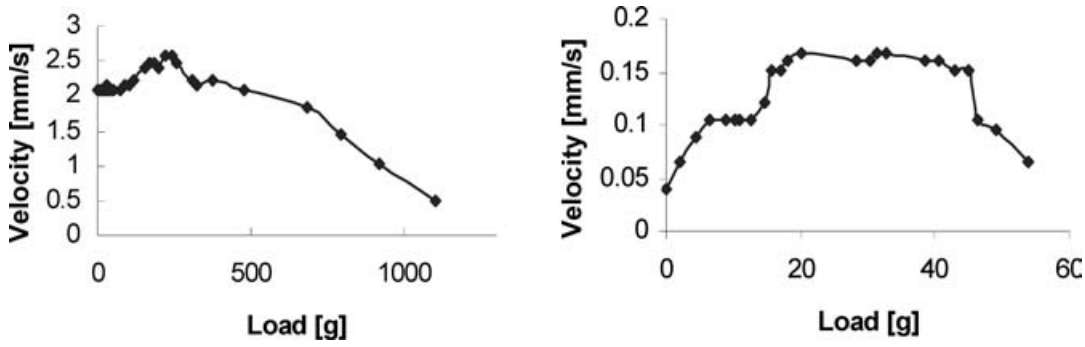


Fig. 8. Velocity of the bigger platform (left) depending on the load on top, compared to the velocity of the smaller platform (right).

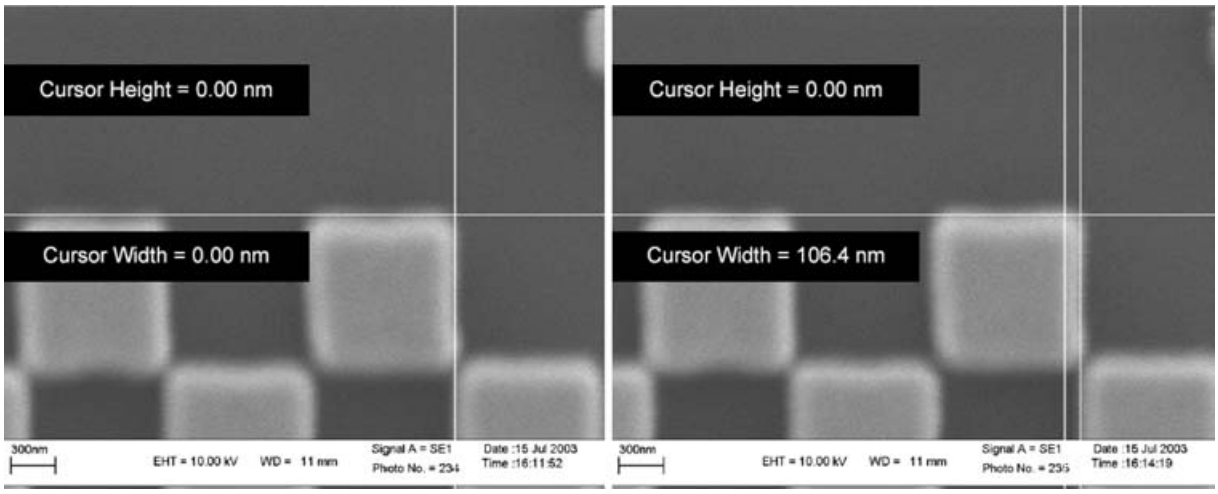


Fig. 9. Minimal step width of the mobile platform RollBot.

49 nF (@1 kHz; 1 V) for the bigger platform and 40 nF (@1 kHz; 1 V) for the smaller platform. So it is reasonable to integrate batteries into the platform. First experiments for the integration of the battery showed promising results. A block diagram of the electrical system is shown in figure 10.

Up to now a PC with an integrated 16 Bit D/A PC-Card plus DSP is generating the sawtooth signals to drive the piezo discs. The dashed block shows the driver unit PCB and consists of a single coil full-wave resonant DC/DC-Converter with integrated high voltage operational amplifiers. Some tests were perfomed to evaluate the potential of the battery integration and to compare different types of batteries. A input sawtooth signal with a frequency $f = 900$ Hz was chosen with $U_{max} = +/-1$ V. The first battery, a Alkaline IEC 6LR61 (9 V/0.5 Ah), offered a operating duration of around 1 h for an output peak to peak amplitude of 40 V, while another set of batteries, the IEC LR6 (3×1.5 V/2.6 Ah), offered an operation of 5 h with a peak to peak voltage of 22 V. The integration is not yet complete, but the experiments have shown that an on-board power supply is feasible. Up to now, the batteries were chosen without consideration of the vacuum of a SEM chamber.

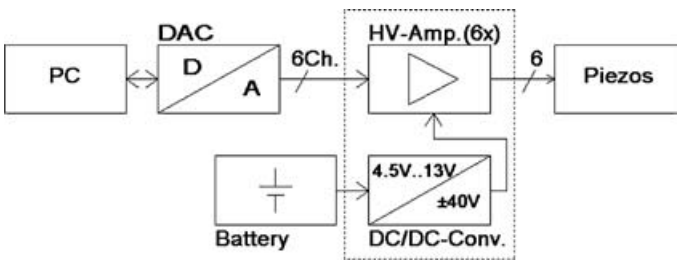


Fig. 10. Block diagram of the battery based driving circuit.

Both types of platforms presented here are useful for a manipulation station. As mentioned before, a microrobot needs more than just a mobile platform. A manipulation unit on top is required as well. Sometimes it is necessary to reach several cm^3 working range for the manipulation unit. In such cases it is useful to choose the platform with a greater contact surface to stabilize the whole mechanical system. In all other cases the smaller platforms are preferred.

2.2. Manipulation unit

The micromanipulator's working distances run from a few μm up to several mm. In some cases the micromanipulator has to work with nanometer accuracy. Because of that, it is necessary to differentiate between coarse positioning mode and fine positioning mode again.

Two different configurations for the manipulator unit are described here. The first one is a manipulator driven by three linear actuators with piezoelectric ceramics as functional material. The second one is driven by a combination of micromotors and piezoelectric ceramics.

https://doi.org/10.1017/S0263574704000852 Published online by Cambridge University Press

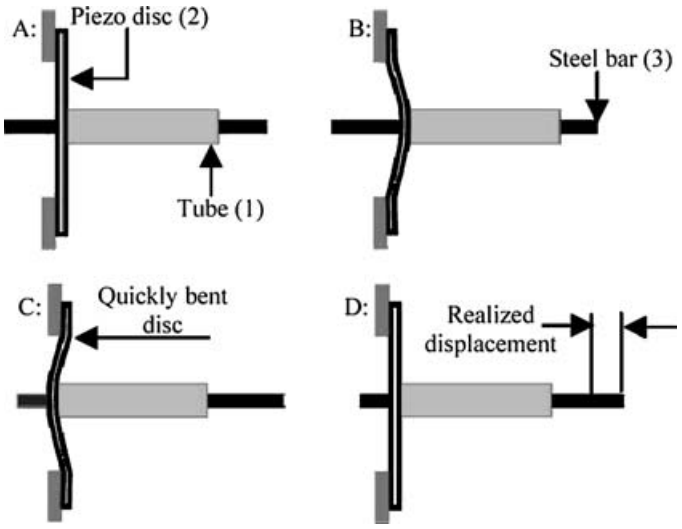


Fig. 11. Slip-stick for the linear actuator.

For the first configuration the driving principle is the slip-stick principle again. The linear actuator is described along with figure 11.

The tube (1) is fixed on an unimorph piezo disc (2). This is he same kind of piezo disc used for the mobile platforms. It is possible to move a jammed steel bar (3) relative to the tube, but this movement requires a defined strength. When the piezo disc gets bent by a voltage, the tube attached to the disc follows the movement. It is possible to realize a fine movement by slowly changing the disc's shape, because the tube with the steel bar follows that movement. But with a quick change of the disc's shape the tube slips along the steel bar, which keeps its position due to inertia. Velocities up to several mm/s have been realized by repeating the small steps in a high frequency. This process is similar to the working principle of the nanomotor®, a product with an accuracy in the sub-nanometer range.[18] A first prototype of a manipulation unit, shown in figure 12, uses three of these linear actuators to realize three DOF, the pitch, roll and linear movement in the z-direction.

In combination with the presented mobile platform, the robot system has 6 DOF without any redundancy. But, as described before, the resolution of the mobile platform is restricted to approximately 110 nm, because the usability of the fine positioning mode has to be checked before. Each of the linear units has a travelling range of 10 mm.

The manipulator platform can be tilted to more than 13°. When a high precision movement is needed, often flexible hinges are used which usually have only a limited range of motion. For the first realized prototypes flexible hinges were used. But these hinges have long settling times. Their strong vibrations cause an instability of the whole manipulator. Therefore alternative joins are used to substitute the flexible hinges.

One micromanipulator, designed for the bio manipulation, uses magnetic joints (figure 13).

This kind of clamp allows the removal of the manipulation platform by hand, without any extra tool. The platform centres itself because of the magnetic force. We have not detected any disturbance caused by the magnetic bearing, like vibrations, or drift, which has any relevance on the precision needed for micromanipulation, e.g. biological cell handling (section 3).

The microrobots which have to work inside a SEM should not use permanent magnets, because ther magnetic field would influence the electron beam. Consequently an alternative clamping system is implemented as well (figure 14). Three pairs of fixing pins are placed with a 120° pitch angle. When the height of the platforms A, B or C is changed, ruby balls can slip along the fixing pins. The resulting slip effect of the breakout force during the movement of the platforms is unproblematic for the microrobot's precision, because it occurs only during the coarse positioning. The fine positioning takes place independently from the coarse positioning unit by controlling the shape of the piezo elements D. In this way the upper platform E is moved relatively to the lower platform F. The platform F and platforms A, B and C are connected by six contact points. Such a clamp fits the modular concept, because it is easy to exchange the upper platform without using a tool.

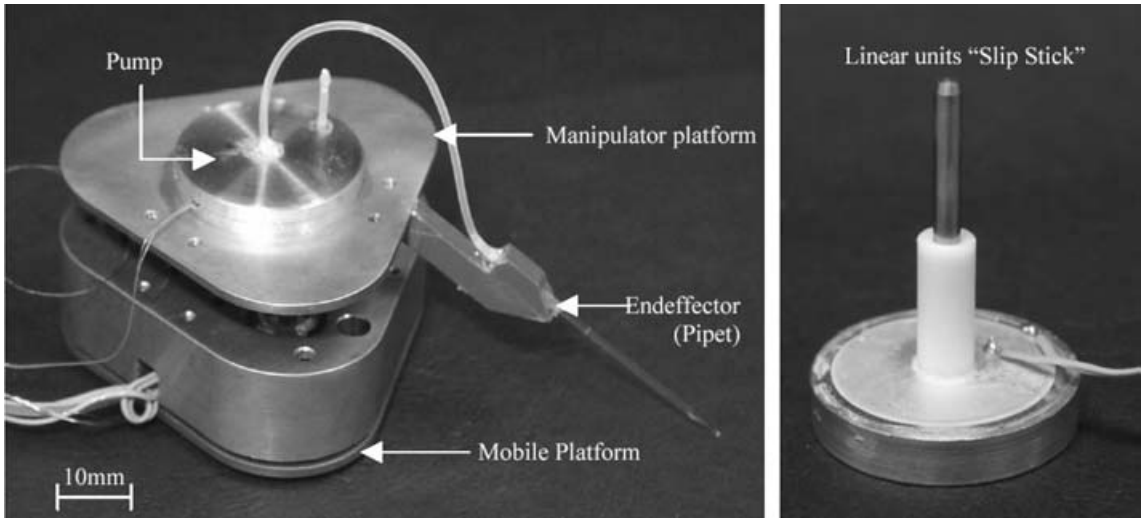


Fig. 12. Microrobot (RollBot V) and its linear actuator, driven by the slip-stick-principle.

https://doi.org/10.1017/S0263574704000852 Published online by Cambridge University Press

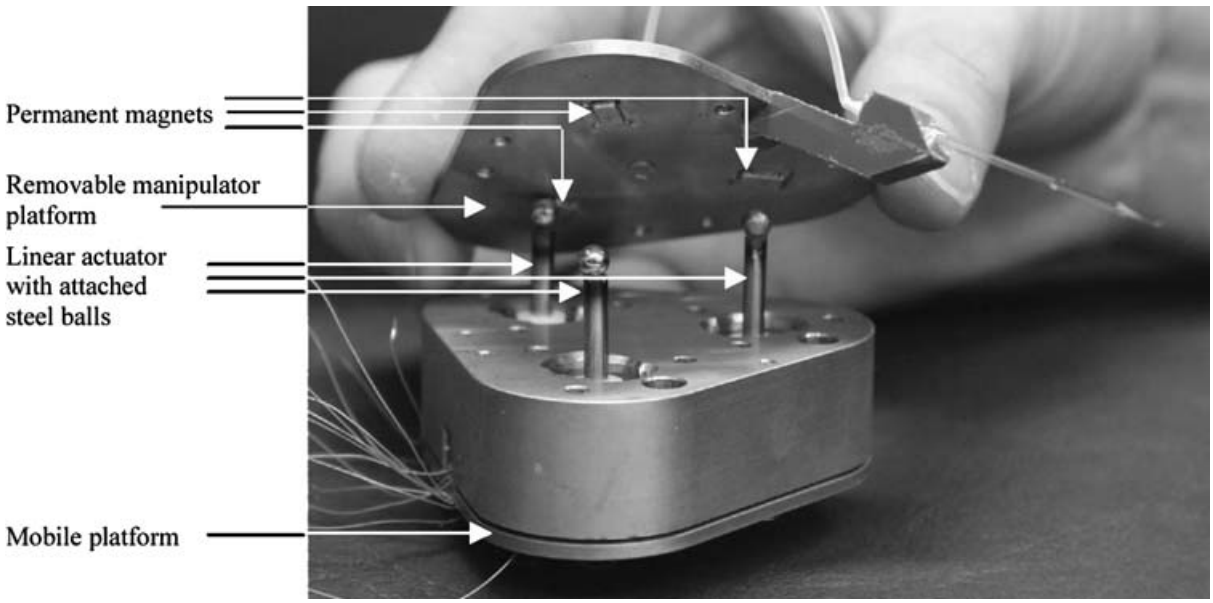


Fig. 13. Removable platform of the RollBot V with magnetic joints.

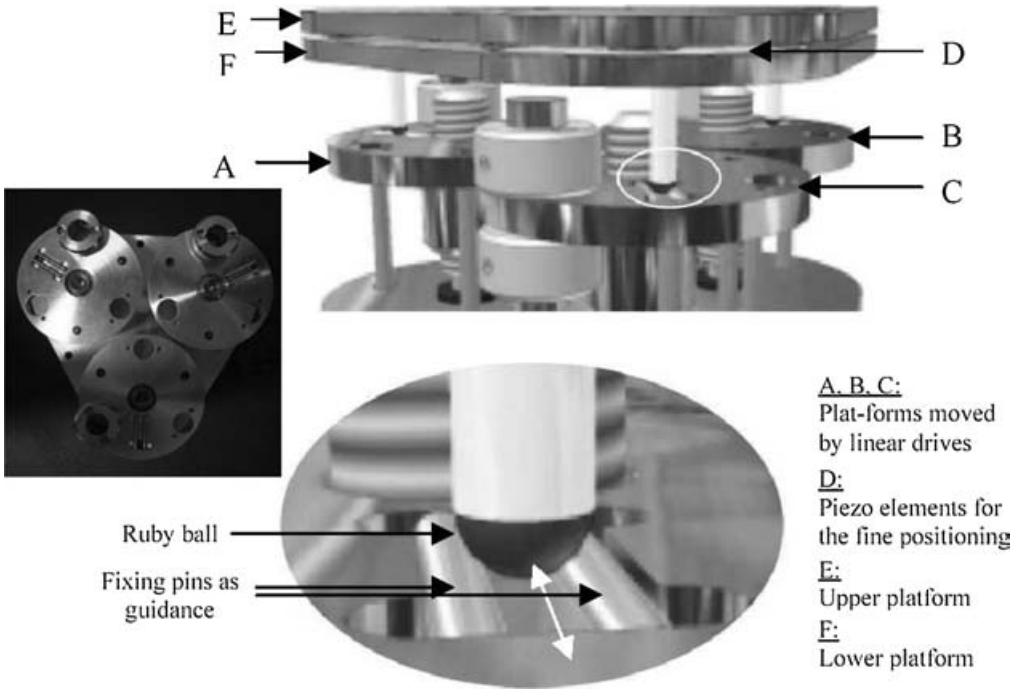


Fig. 14. Kinematic clamp of the manipulator unit.

The piezoelectric linear actuators are able to exert forces of approximately 0.4 N each. That is enough for most micromanipulation tasks. But sometimes the microrobot has to carry heavy end-effectors and equipment. In this cases an alternative driving concept must be implemented. A promising option is the use of micromotors in positioning units. A first prototype is explained here.

The manipulator is driven by a combination of Mymotors' GEC 001 micromotors with TMS 025 spur gears and piezoelectric ceramics (figure 15). The micromotors are used for coarse positioning with a precision of approximately 10 μm. The fine positioning in the nanometer range is performed by piezoelectric ceramics, placed on top of the stages positioned by the micromotors. A compact, but mechanically simple structure has been chosen (figure 16).

The motor (1) is fixed to the mobile platform. It is necessary to use a defined force to move the alignment pins (3) jammed inside guidances (2) in parallel to the micro motors. A fine threaded rod (4), rotated by the micro motor, moves a small table (6) with a screw socket (5). Three of this linear tables are integrated into each micromanipulator. All used alignment pins are fixed to the small tables. Because the pins are jammed, as described before, there is no clearance left. In this way it is possible to load each table, while it keeps

https://doi.org/10.1017/S0263574704000852 Published online by Cambridge University Press

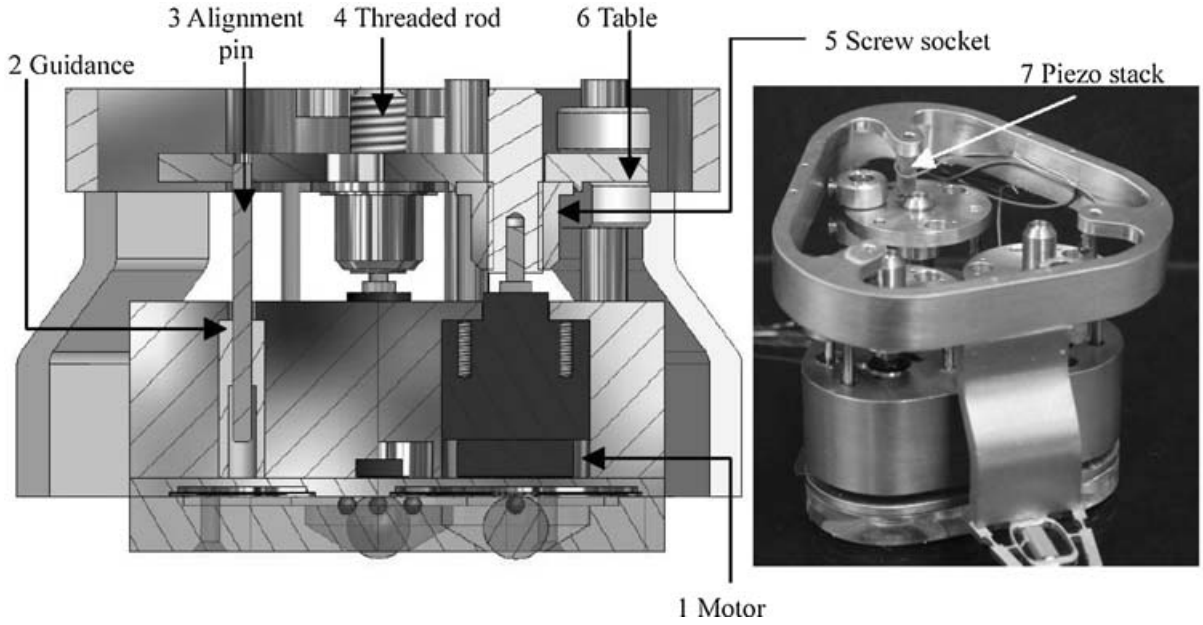


Fig. 15. Driving principle in the linear actuator.



Fig. 16. Mobile microrobot (RollBot IV) with the manipulator unit in two different positions.

its position. By small rotations of the micro motor the table can be positioned with a precision of approximate 10 μm. The level of the three tables, driven by the micromotors, is controlled by the use of three DVRT-sensors (MicroStrain, 8 mm Subminiature DVRT), offering a repeatability of $+/-1$ μm. The piezo stacks (7) are capable of overlapping the few μm while realizing a nanometer precision. Figure 16 and 17 show a mobile microrobot with a manipulator unit driven by a combination of an electromotor and piezoelectric ceramics.

3. HANDLING AND TRANSPORTING OF CELLS

An important application is the handling of biological cells. In microbiology and medical research on the cellular level, it is not feasible to manipulate objects, i.e. cells, without the aid of micromanipulation devices. There is a multitude of possible applications for microrobots in biological cell handling.

The microinjection into living cells is a common task in bio technology. For this, the cell needs to be held in place, while liquids or other particles like spermatozoa are injected with a microcapillary. The cell is usually held pneumatically with a second capillary. This scenario shows the need for multi robot systems. One microrobot is used to hold or transport the cell while the other carries out the injection. In this section, microrobots are shown that are able to hold, lift, and transport cells.

3.1. System setup

Figure 18 shows the robots used. The robot based on RollBot IV works with an external pneumatic microinjector (Eppendorf), while the robot based on RollBot V carries its own micropump, constructed with a piezo disc that can alter

https://doi.org/10.1017/S0263574704000852 Published online by Cambridge University Press

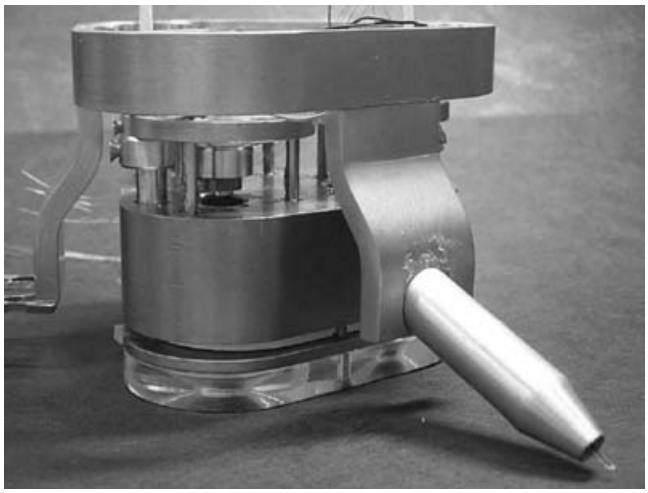


Fig. 17. The same microrobot as above, but with a different tool platform placed on top.

an enclosed volume. The RollBot V has enough mass not to be restricted in its movement by the vacuum hose connected to the external microinjector.

While the automation of such tasks is a research goal, the first goal is to develop a system that is teleoperated by the user. Living cells require very delicate handling. Therefore a haptic interface is of great use for the operator. Such a haptic feedback system is currently being developed (see section 4).

If one wants to develop a successful closed-loop control of the robot's movements, reliable position measurements of the robot and the objects to manipulate are required. In the case of microrobotics, machine vision is often the only sensor available. This makes sophisticated image processing mandatory for position measurements. The coordinate system for the experiments is defined so that the microscope stage is the x-y-plane and the z-coordinate is normal to that plane and parallel to the movement of the focus drive.

The imaging system used in the experiments described below consists of a motorized, inverted microscope (Zeiss Axiovert 200M), a digital CCD color camera fitted to the microscope (Basler A101 fc), and a PC to control microscope and camera, and to run the image processing software. Image processing routines from the Matrox Imaging Library (MIL) were used.

The z-position of the object to be manipulated is determined by an autofocus algorithm that detects and correlates edges in the image. Since the plane of the focus is similar in all experiments – it is determined by the microscope stage's z-coordinate – this autofocusing can be done quickly at the start of the experiment or to find the capillary's z-position again after large movements. The information about the z-coordinate is gathered from the microscope's focus drive controller, which has a sufficient resolution – minimum step size 0.025 μm (manufacturer's specification). If one pessimistically assumes that the repeatability of accurate measurements is one order of magnitude worse, the measurements are still accurate within 250 nm.

After the image is in focus, a geometric model finder algorithm can be used to detect and track the target object, which in case of these experiments is an Expancel sphere – a transparent polymer sphere encapsulating a gas. By applying heat, these spheres can be expanded to various diameters, thus creating test objects with a range of sizes akin to those of typical eukariotic cells.

At the start of the experiment, the z-position of the capillary's tip is unknown, yet for safety reasons far above the target objects' focus plane. That means that the capillary is entirely not in focus and cannot be detected by a geometric model finder algorithm. The z-position can now be determined by a focus scan: the microscope's focus drive moves with a constant velocity and the image is grabbed in defined intervals and its focus index is determined by the focusing algorithm.

At large distances of the end-effector from the object plane, this procedure yields two distinct peaks, representing the object focus plane and the capillary focus position (figure 19, left). It should be noticed that the peaks are narrowing for greater magnification – smaller depth of focus. If the capillary is lowered towards the objects, those peaks merge into one, and therefore the capillary's z-position cannot be reliably determined anymore with this method. Instead, when the capillary is near the object plane, the process that keeps the

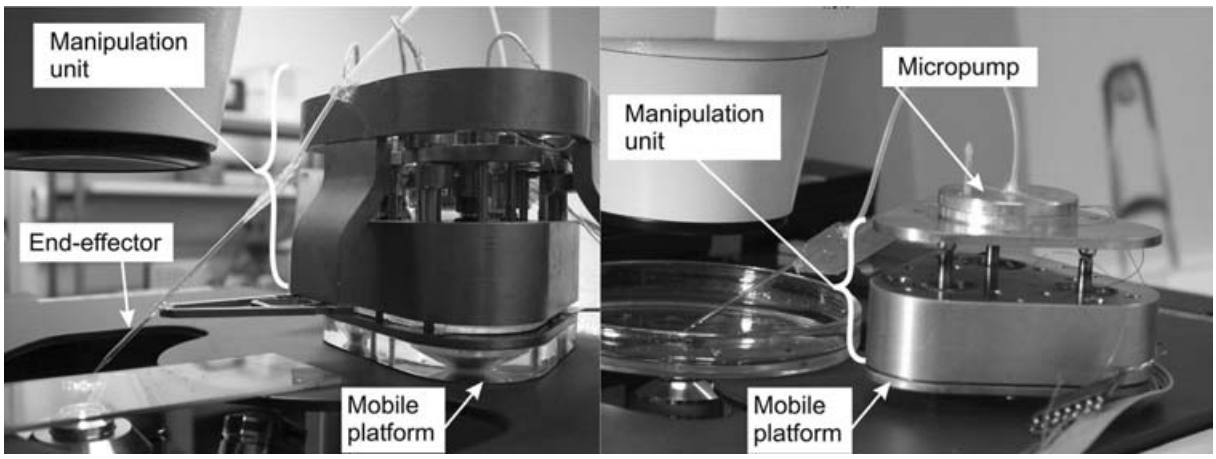


Fig. 18. RollBot IV (left) and V (right) in the CellBot configuration, outfitted with a capillary as end-effector and placed on the stage of an inverted microscope (see also Fig. 12, 13).

https://doi.org/10.1017/S0263574704000852 Published online by Cambridge University Press

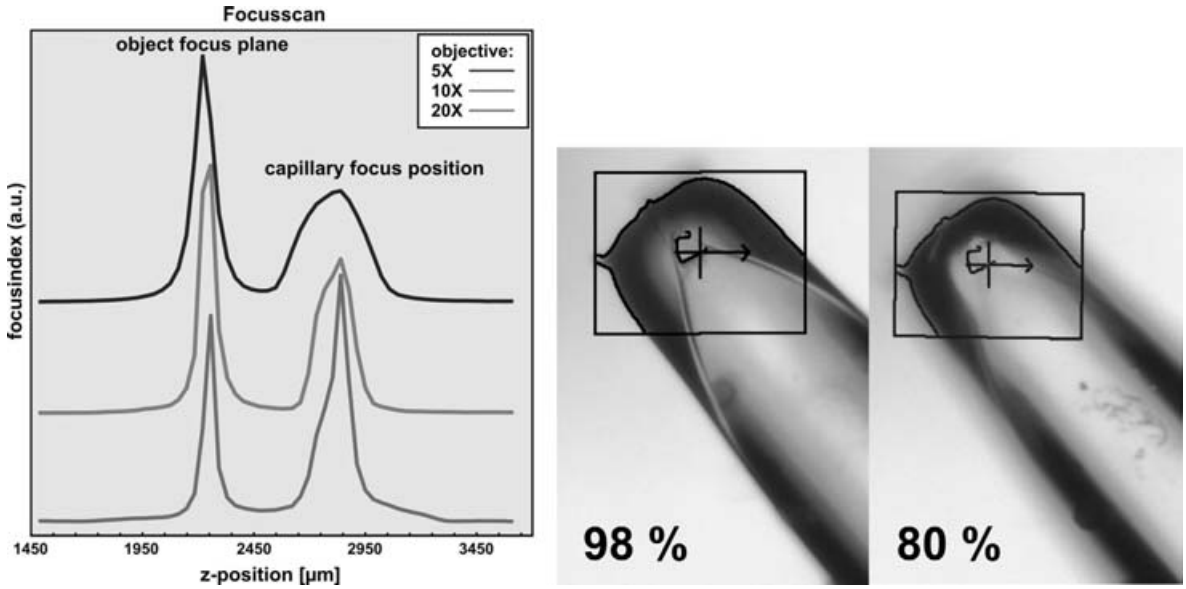


Fig. 19. Different methods of automatic focusing. Left: Focusscan with different objectives; normalized. Right: Capillary in focus and slightly out of focus. The numbers are the correlation between the original model used by the geometrical model finder algorithm and the actual image.

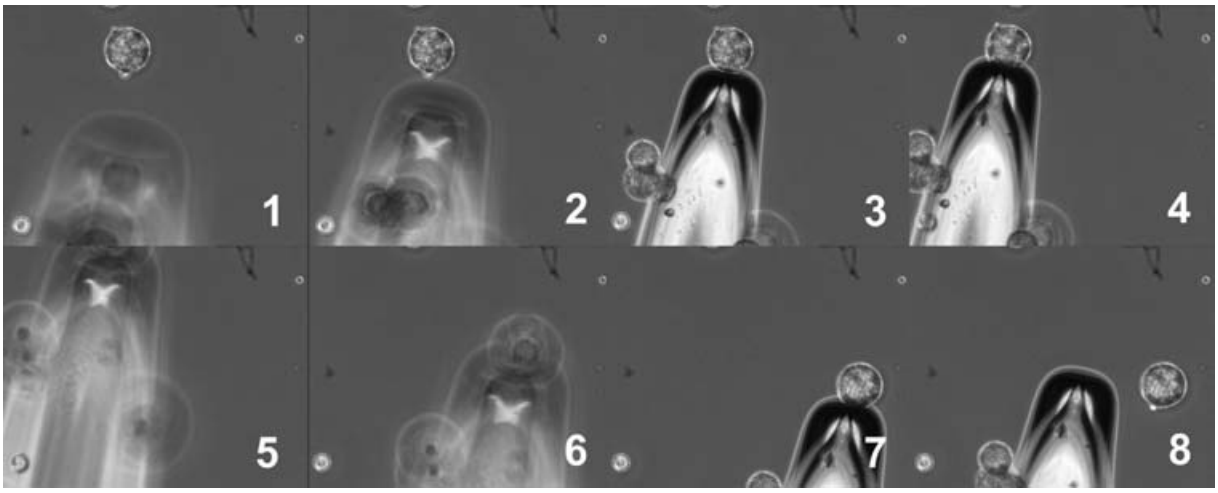


Fig. 20. A sequence of handling with the capillary. The object is lifted, transported to the right, and released.

capillary in focus switches over to using the geometrical model finder algorithm (figure 19, right).

The correlation value put out by the model finder algorithm can be used to determine the sharpness of the capillary in the image, while at the same time disregarding the sharpness of objects with different shapes also in the image. This correlation value is also very sensitive to slight changes of focus of the capillary. Together with the focus drive controller of the microscope, this can be used to determine small deviations of the capillary's z-position from the focus plane of the target object. At the same time, the geometrical model finder is used to determine the pose of the end-effector in the x-y-plane, and is used to implement the trajectory control of the robot.

3.2. Experiments

In this section, an experiment is described in which a sequence of holding, lifting, transporting and releasing an object was executed. Figure 20 shows images from such a sequence.

In this sequence the robot approaches a cell, holds it with the capillary, lifts it out of the focus plane, transports it a short distance and puts it down again. In this figure, the pictures are taken with the object plane always in focus. That means, if the capillary is not focused in the image, it is above the object plane, like in steps 1 and 2 (approaching the target object from above) and 4 and 5 (having lifted the target object and transporting it to the right). In step 3 of the sequence, the capillary is first brought into contact with the object, which is then pneumatically held through steps 4–7. In step 7 the capillary is lowered again to the original object focus plane. And in step 8 the object is successfully released from the tip of the capillary, which is not a trivial task because of the strong contribution of adhesive forces in the microworld. In fact, in the pictured sequence, other objects that adhere to the capillary can be seen.

https://doi.org/10.1017/S0263574704000852 Published online by Cambridge University Press

These experiments use most of the DOF of the robot and show that for all DOF the robot is capable of controlled, precise movement, so that cells can be successfully handled and transported.

4. HAPTIC INTERFACE

Most current concepts for the manipulation and assembly of tiny objects rely mainly on machine vision. However, force and tactile feedback is required for precise, reliable and non-destructive manipulation of microobjects.[19,20]

Different commercially available haptic devices are currently used for the force feedback teleoperation of microrobots, e.g. Phantom, Delta or force feedback joysticks.[3,21–24] These haptic devices were initially designed for virtual reality applications and not for the control of complex robotic systems. Some research groups develop haptic devices for the teleoperation of different micromanipulators.[21,25,26] However, all these haptic interfaces do not enable simple and intuitive teleoperation of microrobots. There are a number of reasons for that:

- Microrobots manipulate objects of different materials and sizes. Gripping forces can range from several millinewton ($\sim 10^6$ nN) down to tens of nanonewton ($\sim 10^1$ nN). This means that the estimated ratio of maximal force to minimal force used in microrobotics is around 10^5:1. However, existing haptic interfaces have much lower dynamic range of forces and therefore can't effectively represent the whole range of forces that occur in microrobotics applications.
- Existing mobile microrobots have a nanometer resolution of motion. At the same time they have a practically unlimited working area. Usually, when working under a light microscope or in an SEM chamber, the working area of microrobots is limited to several centimetres ($\sim 10^8$ nm). This means that the ratio between working area and motion resolution of microrobots is 10^8:1. However, existing haptic interfaces have much lower ratio of workspace to motion resolution. That is why additional input devices like keyboards or mice are used together with them to adjust the scaling factors. This slows down the teleoperation of microrobots and complicates user interfaces. To get rid of this drawback an ideal haptic device should have integrated buttons to easily adjust speed of a microrobot or a scaling factor between the motion of a haptic device and a microrobot.
- Signals from a force microsensor integrated into the gripper of a microrobot consist of not only static force components but also low and high frequency force components which carry information about the working state of the microrobot, the state of a grasped object or a microhandling process. The bandwidth of a force signal can range up to several kHz. The existing haptic interfaces have much a lower bandwidth and therefore can not effectively represent microforces to an operator.
- Many microrobots have an end-effector in the form of a gripper with a force microsensor. To control this end-effector an ideal haptic device should have a corresponding active 1 DOF gripper handle. Unfortunately most haptic interfaces have no such gripper handle.
- The complex control of a microrobot requires switching the microrobot between different modes and indicating the working state of the microrobot. To realise that, an ideal haptic device should have integrated control elements (buttons and light indicators).
- It is seldom necessary to move microrobots (by humans in teleoperated mode) simultaneously in three or more DOF, because such a complex motion doesn't provide fast and precise positioning. That is why an ideal haptic interface should provide the ability on a user request to decouple the motions in different axes and to assign each DOF of the haptic device to a different DOF of the microrobot. The existing haptic devices don't provide such features and require the application of special software and hardware solutions.
- For complex microhandling and microassembly tasks it is often necessary to control two microrobots simultaneously with two haptic devices. Therefore an ideal haptic device should be a comfortable interface, which should allow teleoperation of a microrobot by one hand without the need of any additional devices.
- In many cases it is required to perform simple teleoperation of a microrobot under a light microscope where complex automatic control and coordination of many microrobots is not required. In such cases there is no need to use a PC for the control of a microrobot. Thus the performance-to-price ratio of the system will be improved and the complexity of the system will be reduced if it is possible to connect a haptic device directly to a microrobot and run software for the teleoperation of the microrobot directly on the microcontroller of the haptic device. Therefore an ideal haptic device should preferably have an integrated microcontroller capable of teleoperation of microrobots. Unfortunately existing haptic interfaces do not have such integrated microcontrollers.

To overcome the drawbacks of existent haptic devices presented above we develop in our institute the Haptic Interface for a Microrobot Cell (HIMiC) for the teleoperation of microrobots inside an SEM and under a light microscope.

The HIMiC introduces an unique mechanical design, which was specially developed for the comfortable teleoperation of microrobots with different end-effectors. A number of buttons and light indicators were integrated into the HIMiC to allow comfortable teleoperation of microrobots in different operation modes and over a great range of velocities and distances. The HIMiC provides sound feedback, which is used in combination with force feedback to increase the dynamic range of representing forces. The HIMiC has an integrated microcontroller capable of teleoperation of microrobots. The HIMiC is a unique haptic device, which contains all the necessary elements and controls for the teleoperation of microrobots over RS-232 and Ethernet interfaces. On one hand the HIMiC can be effectively used as an independent stand-alone haptic device for the teleoperation of microrobots. On the other hand the HIMiC can be easily integrated into complex microrobots control systems. When designing the HIMiC a low price was taken into consideration. The HIMiC is designed primarily from off-the-shelf components. The total price of HIMiC is around 1,000 USD.

https://doi.org/10.1017/S0263574704000852 Published online by Cambridge University Press

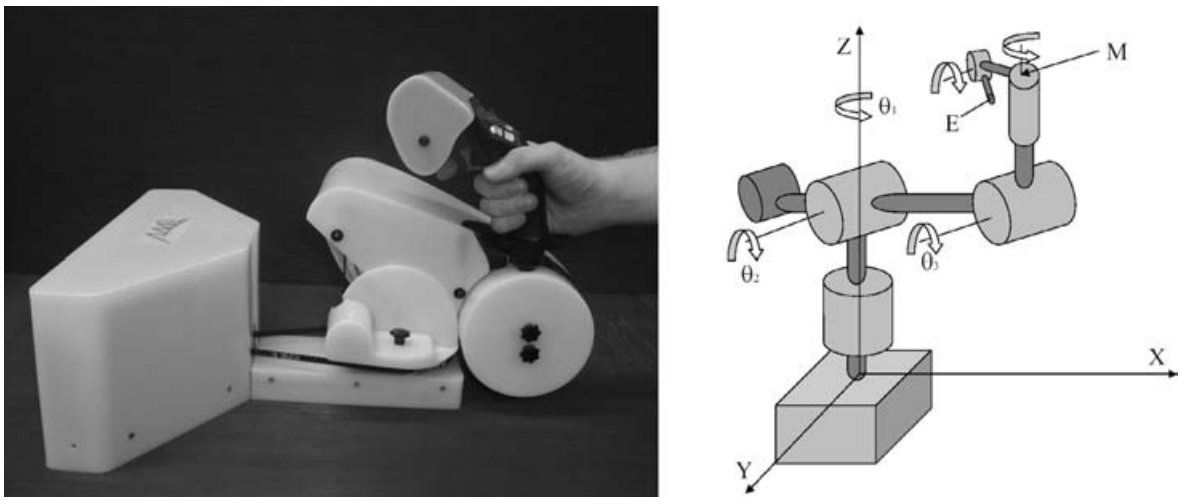


Fig. 21. HIMiC.

First the mechanical design and control system of the HIMiC is described. After that an application of the HIMiC for the force feedback teleoperation of microrobots in an SEM chamber is presented.

4.1. Design of HIMiC

4.1.1. Mechanical design. The HIMiC is being developed to meet the requirements presented above. The prototype of HIMiC and its kinematic structure are shown in Fig. 21.

The haptic device's mechanism is driven by four DC-motors. The mechanical structure provides very little backlash and possibility to decouple motion in different axes. Structural stiffness is more than 7 N/mm, the backdrive friction force less than 0,2 N and the force bandwidth exceeds 50 Hz.

In the haptic device an incomplete gravity compensation has been implemented, so that a user feels approximately 3 N force when moving the haptic handle in Z-axis. At the same time, if the haptic handle is in its lowest position and the user moves the handle only in the X and Y axis, the user does not feel the gravity. This mechanical construction allows more comfortable teleoperation of microrobots. At the same time, it should be pointed out that active gravity compensation is possible whenever it is necessary.

The angular workspace of the HIMiC is $130^\circ \times 60^\circ \times 125^\circ$ (for angles θ_1, θ_2 and θ_3 correspondingly). When moving the handle of the HIMiC, the point M at the tip of its handle describes an arc with the corresponding lengths of $820 \times 370 \times 480$ mm.

The end-effector (E) of the haptic device, which is realised in the form of a 1 DOF active gripper handle, is used to sense motion of a index finger and apply force to it. Usually the motion of this end-effector corresponds to the motion of the microrobot's gripper. The moving angle of the end-effector is 180°. During its motion the end-effector describes an arc with an approximate length of 80 mm.

The torque of the actuators is provided by three 90 W DC-motors from Maxon, which are used for the X,Y and Z DOF, and one 25 W DC-motor, which is used for the end-effector. The torque transmission is realised by using belt and gear wheel transmission. Digital MR encoders from Maxon, mounted on the motor shaft, measure the motion of the motors. Using these encoders it is possible to transmit 4096 counts per revolution resulting in an accuracy of 0,000213 rad when multiplied with the ratio of the transmission 7,2:1. That results in an average position resolution in the workspace 0,04 mm.

On the rear part of this plate all indicators and all electronic components along with one of the dc motors are mounted.

4.1.2. Control system design. To make the haptic device most suitable for the teleoperation of microrobots the computer control system should meet the following requirements:

- Real time operating system for the control of the haptic device and the teleoperation of microrobots;
- Fast DSP capable of simultaneously controlling the haptic device and a microrobot with an update rate up to 100 Hz;
- RS-232 and Ethernet interfaces for the communication with a user PC and a microrobot controller;
- Simple development of applications for the control of the haptic device and for the teleoperation of microrobots;
- Low price of the computer control system.

To meet these requirements the IPC@CHIP SC12 microcontroller (BECK) was chosen for the core of the computer control system. This microcontroller's feature list made it the ideal solution for the haptic device:

- 20 MHz, 16 bit 186 CPU, 512 KB RAM, 512 KB Flash, 10 BaseT Ethernet interface, two RS-232 interfaces, 2 programmable timers, watchdog and power failure detection integrated into one chip;
- The IPC@CHIP SC12 is a combination of hardware and preinstalled software. The software consists of a Real Time Operating System (RTOS) with file system, TCP/IP stack and hardware interface layer.

The architecture of the computer control system and electronic circuit of the HIMiC is shown in figure 22. Two quadruple differential line receiver chips MC3486 are used to read the state of the incremental encoders, which is necessary to calculate the current position of the haptic handle. This step can be implemented by using either a special chip,

https://doi.org/10.1017/S0263574704000852 Published online by Cambridge University Press

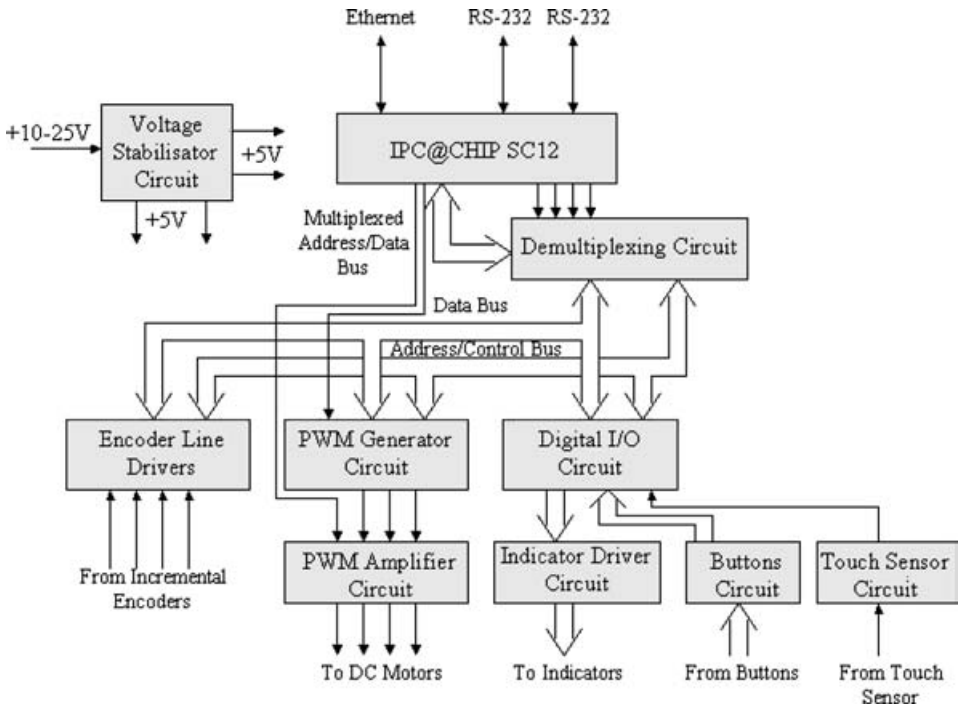


Fig. 22. Architecture of the HIMiC's electronic circuits.

e.g. HCTL-2020, or a microcontroller. The latter solution has been implemented because of the following reasons:

- The velocity of the haptic device's handle is rather slow and calculation of the encoder position by software gives good results
- The software solution reduces the price of the haptic device.

The encoder position is calculated with an update rate of 7 KHz. Three channels of the PWM generator circuit are based on the programmable timer chip CP82C54 that communicates directly with the microcontroller via the address/data bus. One of the microcontroller's timers is used as a 2.5 MHz clock frequency generator; which supplies clock to the timer chip CP82C54. The other timer of the microcontroller sends a PWM signal to a PWM amplifier. PWM amplifiers are based on four full bridge motor drivers with a maximum peak current of 5A for each channel and a maximum output voltage of 40 V. These PWM amplifiers drive the DC-motors. The HIMiC uses open loop force control. An infrared touch sensor is integrated into the handle of the haptic device. Force feedback is activated only when an operator grasps the handle of the haptic device which is signalled by the infrared touch sensor. The control system of HIMiC is capable to run the overall control loop (microrobot + haptic) with an update rate up to 100 Hz.

The control software can be developed on a user PC and then downloaded via FTP to the flash memory of the HIMiC.

4.2. Control architecture of the micromanipulation station

4.2.1. Hardware architecture. Figure 23 gives an overview of the SEM based nanohandling station that is being developed. In the nanohandling station three different types of microrobots are currently used: Microrobot A [27] and B [28] and RollBot/CellBot microrobots can be teleoperated inside an SEM chamber. Simultaneous teleoperation of two microrobots is possible by means of a force feedback joystick and the HIMiC. A force microsensor is fixed to the Microrobot B. This force sensor has an end-effector in the form of a needle. Using the HIMiC, a user can feel forces which act on this force microsensor during the nanohandling procedures.

The control structure of the SEM based nanohandling station is shown in figure 24. The nanohandling station is based on a LEO-1450 scanning electron microscope. A conducting glass plate is mounted on the positioning table inside the SEM chamber. Each of the microrobots has three DOF and operates with an accuracy down to a few nanometers. The SEM provides visual information from the working place of the robots, with a resolution of up to 3–4 nm.

The SEM is controlled by an SEM PC, which acquires the SEM images and displays them on its monitor. The SEM is additionally controlled by the user PC through a RS-232 serial interface. The high-level control software that is responsible for the overall nanohandling station runs on the user PC.

The user PC controls movements of the SEM positioning table, as well as magnification, focus and position of the electron beam. The actuators and position measuring systems of the station's microrobot are connected directly to the microrobot controller which communicates with the user PC via Ethernet. The operator uses the graphical user interface (GUI) on the user PC, the HIMiC and the FF joystick to teleoperate the microrobots, to control the motion of the positioning table in the SEM, and the electron beam of the SEM.

The 6-axis force/torque sensor Nano 17 F/T from ATI Industrial Automation is fixed to the microrobot B. This force sensor has an end-effector in the form of a needle. A force acts

https://doi.org/10.1017/S0263574704000852 Published online by Cambridge University Press

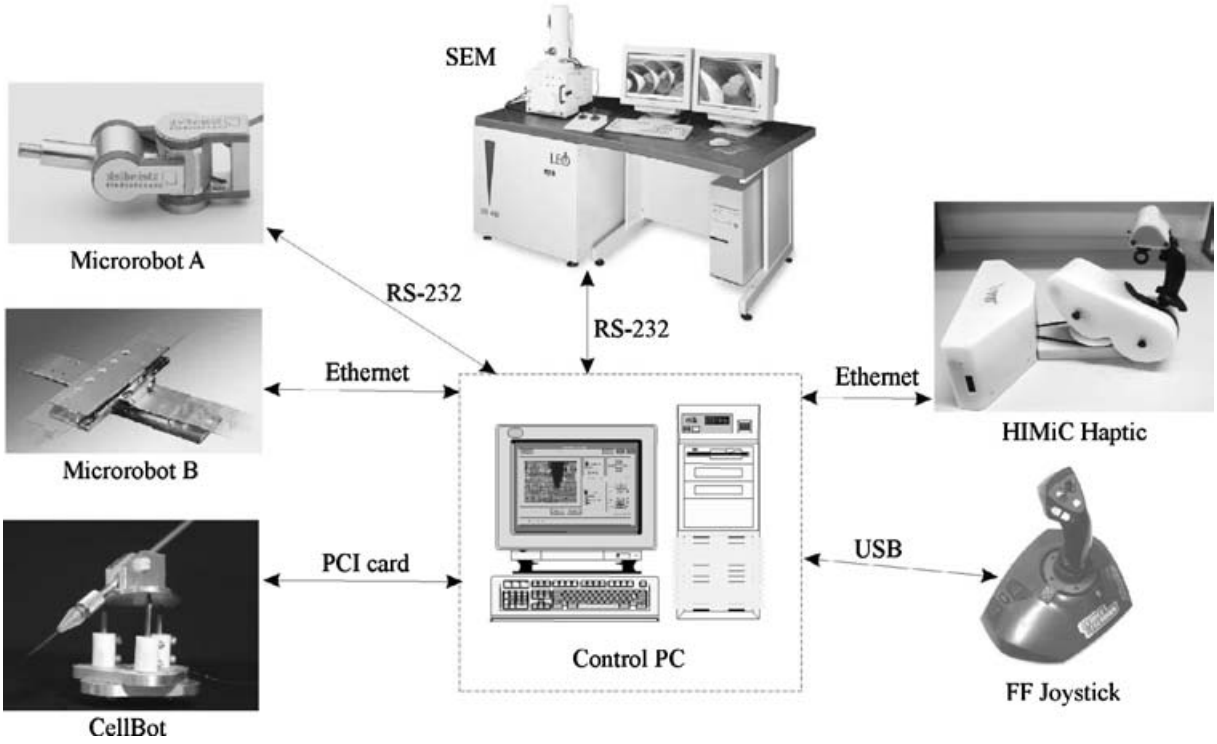


Fig. 23. Overview of the SEM based nanohandling station.

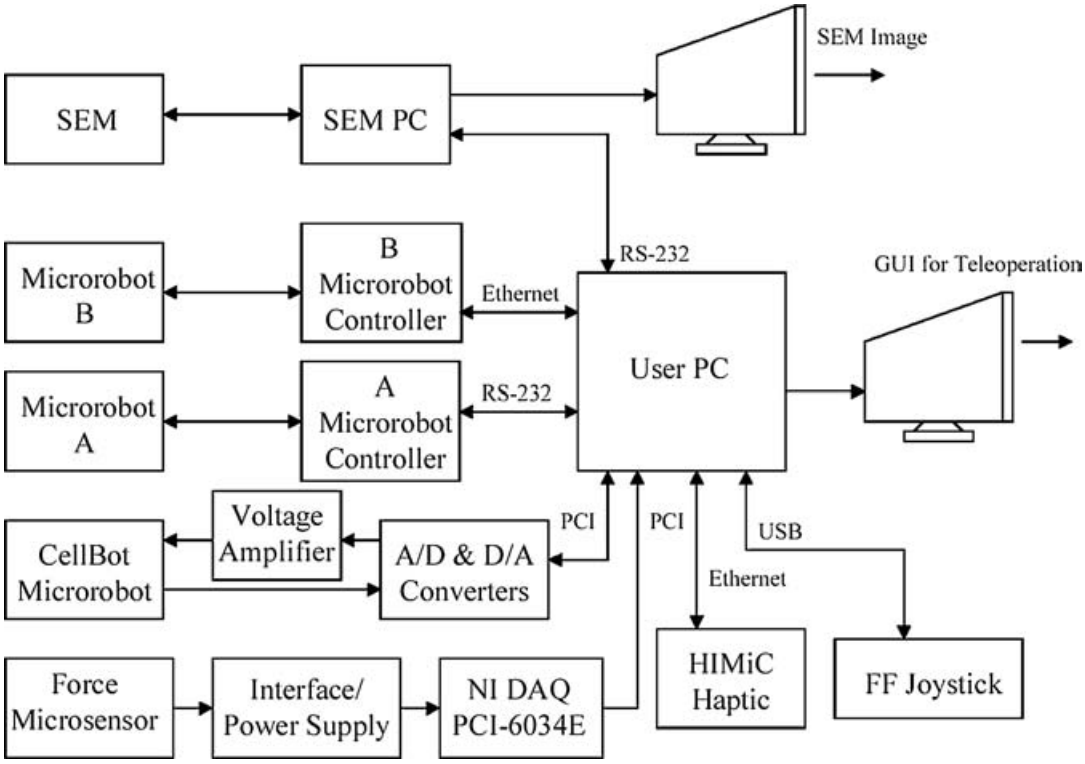


Fig. 24. Control structure of the SEM based nanohandling station.

upon the force sensor when the needle touches microobjects. The upper limit of this sensor is 12 N, the force resolution is 1 mN. The force information from the Nano 17 F/T force sensor is filtered and amplified in the user PC and then sent to the haptic device. The force scaling factor, which is used in the system at this point of development, is 100.

Using buttons on the handle of HIMiC, the user can choose between coarse and fine positioning modes. Since two haptic devices are used for the teleoperation of three microrobots, the user switches between teleoperation of microrobots A and B using one of the HIMiC's buttons. The RollBot is teleoperated using the FF joystick. For the

https://doi.org/10.1017/S0263574704000852 Published online by Cambridge University Press

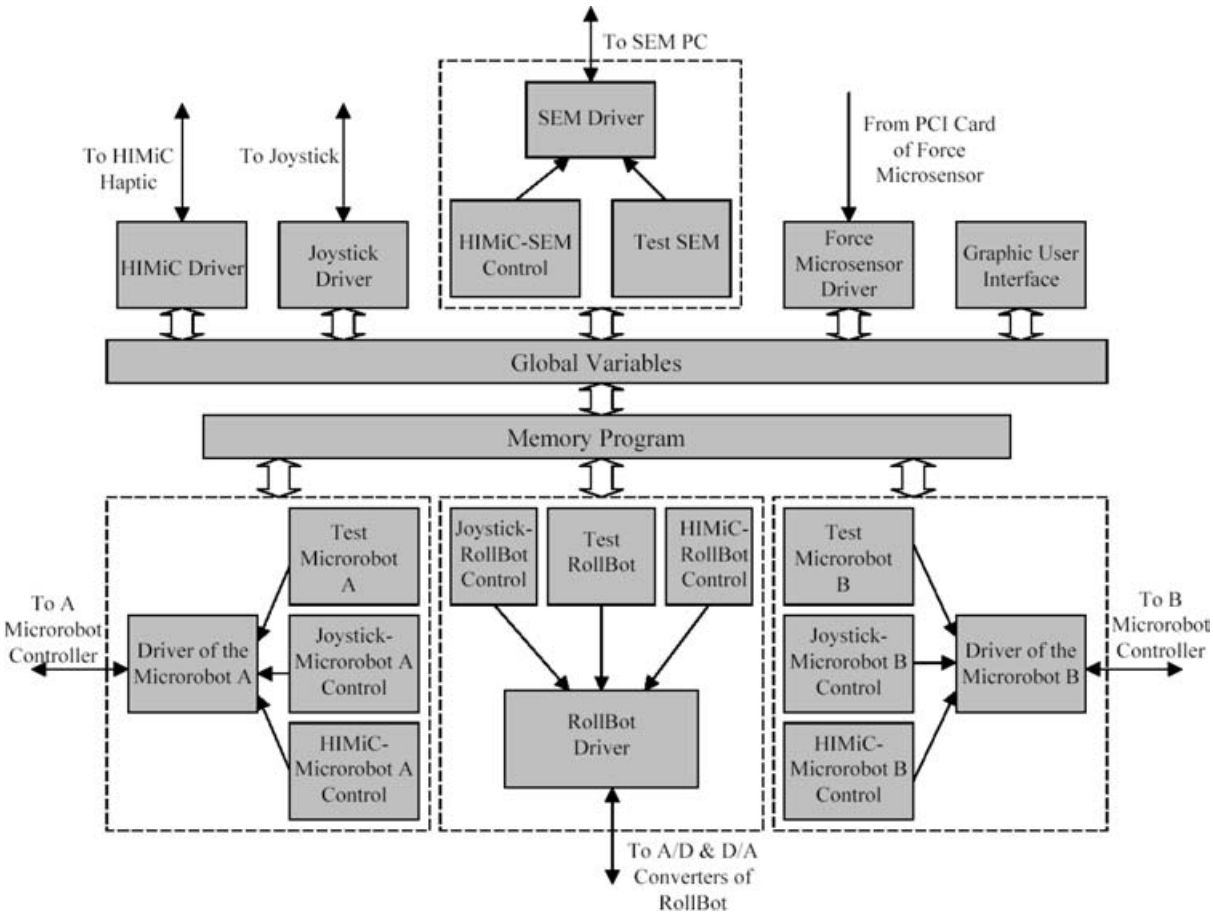


Fig. 25. Control software architecture of the SEM based microhandling station.

coarse positioning the user can choose between the following position scaling factors: 1:1, 10:1, 100:1, 1,000:1. In the fine positioning mode the user can choose between the following position scaling factors: 1000:1, 10,000:1, 100,000:1 and 1,000,000:1. Position scaling factor 1,000,000:1 means that 1 mm of motion of HIMiC's handle corresponds to the 1 nm of motion of a microrobot.

To reduce unwanted motions of the microrobots, the haptic devices send commands to microrobots only if the activation buttons on the haptic handles are pressed. The force feedback of the HIMiC is only activated if the user grasps the handles of the device and activates the infrared touch sensor, as described above.

4.2.2. Software architecture. The control software architecture of the SEM based nanohandling station is shown in figure 25. Each block in figure 25 represents a separate LabView or C++ program. All these programs are then integrated into an overall control program which runs on the user PC. All these programs run in parallel and communicate with each other. The whole microhandling station is controlled from the graphical user interface. From the system configuration menu the operator can choose the device to control. In the operation environment menu the operator can choose between the SEM and the light microscope. The operator can choose between a Wingman Strike Force 3D joystick and the HIMiC. By means of the 'System Testing' menu the operator can verify the correct operation of different components of the microhandling station. The developed teleoperation interface has also three memory functions: teaching, executing and repeating. Using these functions it is possible to save the performed microhandling operation and then play it back from memory, one time or repeatedly. The operator can save to or load from file different microhandling operations.

5. SUMMARY AND OUTLOOK

Within this paper the conception of mobile microrobots has been explained. The main concepts of mobile microrobots were shown. Thereafter a newly developed mobile platform with an innovative drive concept has been described. Because of the configuration of the components for the mobile platforms the integration of batteries for the internal power supply is feasible, as shown by some experimental data. The main characteristics of the mobile platforms has been shown as well. The second major component of a mobile microrobot is a manipulation unit, placed on top of the mobile platform. Two first manipulation units are introduced which need further development. A big challenge will be the further miniaturization of the manipulation unit. To substitute all wires running to or from the microrobot a wireless communication must be implemented.

The robots described in this paper have been used to conduct experiments in the field of cell handling and transporting. These experiments have been fully teleoperated, with some sensor feedback and support by means of image

https://doi.org/10.1017/S0263574704000852 Published online by Cambridge University Press

processing. In the future, further automation of these manipulation tasks will be developed, beginning with closed loop motion control of the robot and leading to automated cell recognition and distinction.

The design of the HIMiC, which is used for the teleoperation of microrobots, has been presented. The requirements that a haptic device should meet have been introduced. On the basis of these requirements the mechanical and control structure of the HIMiC has been developed. The HIMiC was successfully tested by means of the teleoperation of microrobots – two commercially available microrobots as well as microrobots developed by our institute. The integration of the haptic device into an overall control system of a nanohandling station that includes a SEM was discussed.

Future work regarding the development of the haptic interface will include the improvement of sound feedback, which will be used to increase the bandwidth of the haptic system. The next requirement will also include the integration of HIMiC into the multimodal control interface of a microrobot cell, which is currently being developed.

Acknowledgments

The research work is being supported by the German Federal Ministry of Education and Research – VDI/VDE-IT (Joint research project "REMROB", 16SV1383) and by the European Union, project ROBOSEM (GRD1-2001-41864). Financial support is gratefully acknowledged.

References

1. I. Shimoyama, "Scaling in microrobotics", *IEEE/RSJ Int. Workshop on Intelligent Robots and Systems*, Pittsburgh, Penn. (1995) pp. 208–211.
2. H. Morishita and Y. Hatamura, "Development of Ultra Precise Manipulator System for Future Nanotechnology", *Proc. of the Int. IARP Workshop on Micro Robotics and Systems*, Karlsruhe (1993) pp. 34–42.
3. D.-H. Kim, K. Kim, K.-Y. Kim and S.-M. Cha, "Dexterous Teleoperation for Micro Parts Handling based on Haptic/Visual Interface", *Proceedings of the IEEE International Symposium on Micromechatronics and Human Science*, Nagoya, Japan (2001) pp. 211–217.
4. W. Zesch, R. Büchi and R. Siegwart, "Inertial mechanisms for positioning microobjects: Two novel mechanisms", *SPIE Conf. on Microrobots and Micromechanical Systems*, Philadelphia, USA (1995) pp. 80–88.
5. H. Bleuler, R. Clavel, J.-M. Breguet, H. Langen and E. Pernette, "Issues in Precision Motion Control and Microhandling", *Proc. of the 2000 IEEE International Conference on Robotics & Automatisation*, San Francisco, CA (2000) pp. 959–964.
6. A. Codourey, M. Rodriguez and I. Pappas, "A Task-oriented Teleoperation System for Assembly in the Microworld", *Proc. of ICAR'97 Int. Conf. On Advanced Robotics*, Monterey, USA (1997) pp. 235–240.
7. R. S. Ruoff, "Nanomanipulation and Characterisation of individual Carbon Nanotubes", *International Conference on Computational Nanoscience and Nanotechnology* (ICCN 2002), Puerto Rico, USA (2002) pp. 263–270.
8. L. Dong, F. Arai and T. Fukuda, "3D Nanorobotic Manipulations of Multi-Walled Carbon Nanotubes", *Proc. of the 2001 IEEE Int'l Conf. on Robotics and Automation* (ICRA 2001), (2001) Vol. 1, pp. 632–637.
9. M. Falvo, R. Superfine, S. Washburn, M. Finch, R. M. Taylor, V. L. Chi and F. P. Brooks, "The Nanomanipulator: A Teleoperator for Manipulating Materials at the Nanometer Scale", *Proc Int. Symp. on Science and Technology of Atomically Engineered Materials*, Singapore (1996) pp. 579–586.
10. S. Fatikow, B. Magnussen and U. Rembold, "A Piezoelectric Mobile Robot for Handling of Microobjects", *Proc. of the International Symposium on Microsystems, Intelligent Materials and Robots* (MIMR), Sendai (1995) pp. 189–192.
11. J.-M. Breguet, E. Pernette and R. Clavel, "Stick and slip Actuators and parallel architectures dedicated to microrobotics", *Microrobotics: Components and Applications*, SPIE's Photonics East, Boston (1996) Vol. 2906, pp. 13–24.
12. W. Zesch, R. Büchi and R. Siegwart, "Inertial Drives for Micro- and Nanorobots: Two novel mechanisms", *SPIE Conf. on Microrobots and Micromechanical Systems*, Philadelphia, USA (1995), pp. 80–88.
13. H. Wörn, J. Seyfried, S. Fahlbusch, A. Bürkle and F. Schmoeckel, "Flexible Microrobots for Micro Assembly Tasks", *Int. Symposium on Micromechatronics and Human Science* (HMS 2000), Nagoya, Japan (2000) pp. 135–143.
14. S. Martel, K. Doyle, G. Martinez, I. Hunter and S. Lafontaine, "Integrating a complex electronic system in a small scale autonomous instrumented robot: the NanoWalker project", *Proc. of SPIE, Microrobotics and Microassembly*, Boston (1999), Vol. 3834, pp. 63–74.
15. U. Simu and S. Johansson, "Fabrication of monolithic piezoelectric drive units for a miniature robot", *Journal of Micromechanics and Microengineering* (2002) pp. 582–589.
16. L. Juhas, A. Vujanic, N. Adamovic, L. Nag and B. Borovac, "Development of Platform for Micro-Positioning actuated by Piezo-Legs", *Proc. of the 2000 IEEE, Int. Conf. on Robotics & Automatisation*, San Francisco, CA (2000) pp. 3647–3653.
17. S. Fatikow, J. Seyfried, St. Fahlbusch, A. Buerkle and F. Schmoeckel, "Development of a Microrobot-Based Microassembly Station", *Proc. of 9th Int. Conference on Advanced Robotics* (ICAR), Tokyo (1999) pp. 205–210.
18. V. Klocke, "Trends in Nanomanipulation: From Nanomotor to Micro Production Line", *Proc. ACTUATOR 2002*, Bremen (2002) pp. 100–105.
19. Y. Zhou and B. J. Nelson, "Force Controlled Microgripping", *Microrobotics and Microassembly, Proc. of SPIE* (1999) Vol. 3834, pp. 211–221.
20. S. Fahlbusch, A. Shirinov and S. Fatikow, "AFM-based Micro Force Sensor and Haptic Interface for a Nanohandling Robot", *Proc. of IEEE/RSJ Int. Conference on Intelligent Robots and Systems*, Lausanne, Switzerland (2002) pp. 1772–1777.
21. N. Ando, M. Ohta and H. Hashimoto, "Micro Teleoperation with Parallel Maniulator", *Proc. of the 2000 IEEE/RSJ International Conference on Intelligent Robotics and Systems*, Japan (2000) pp. 677–682.
22. E.-H. Song, D.-H. Kim, K. Kim and J. Lee, "Intelligent User Interface for Teleoperated Microassembly", *Proc. of the 2001 International Conference on Control, Automation and System*, Korea, October (2001) pp. 784–788.
23. M. Falvo et al., "The nanomanipulator: A teleoperator for manipulating materials at the nanometer scale", *Proc. of the Int. Symposium on the Science and Technology of Atomically Engineered Materials*, Richmond (1995) pp. 579–586.
24. S. Grange et. al., "The Delta Haptic Device as a nanomanipulator", *Proc. of SPIE Int. Conf. On Microrobotics and Microassembly*, Boston, USA (2001) pp. 100–111.
25. N. Ando, M. Ohta and H. Hashimoto, "Micro Teleoperation with Haptic Interface", *Proc. of the IEEE International Conference on Industrial Electronics, Control and Instrumentation* (IECON 2000), (2000) pp.13–18.
26. M. Goldfarb and J. Speich, "Compliant Micromanipulator Design for Scaled Bilateral Telemanipulation of Small-Scale Environments", *ASME International Mechanical Engineering Conference and Exposition* (1998) DSC-Vol. 64, pp. 213–218.

https://doi.org/10.1017/S0263574704000852 Published online by Cambridge University Press